Inflammation, Vol. 45, No. 3, June 2022 (© 2022)
https://doi.org/10.1007/s10753-021-01618-5

ORIGINAL ARTICLE

Human Breast Milk–Derived Exosomal miR-148a-3p Protects Against Necrotizing Enterocolitis by Regulating p53 and Sirtuin 1

Miao-miao Guo[1] , Kun Zhang[1] and Jia-hui Zhang[1,2]

Received 11 August 2021; accepted 17 December 2021

Abstract—Necrotizing enterocolitis (NEC) is a gastrointestinal disease that results in the exaggerated intestinal inflammation and injury. Human breast milk–derived exosome (BM^{EXO}) has been reported to relieve NEC, which is closely related to the contained microRNAs (miRNAs). However, which miRNA and whether its synthesized mimic can replace the protection of BM^{EXO} remains unclear. We established a NEC mouse model, and miRNA sequencing was performed to determine the miRNA profiling in BM^{EXO}. The downstream target of miRNA was then confirmed by dual-luciferase reporter assay. Finally, we explored the protective effect of a single miRNA agomir on NEC and its downstream mechanisms. The results revealed that BM^{EXO} treatment exerts a significant protective effect on NEC mice, including inhibiting inflammation and improving intercellular tight junctions. Additionally, as the most abundant miRNA in BM^{EXO}, miR-148a-3p directly targets *Tp53* on its 3′ untranslated region (3′ UTR). miR-148a-3p mimic treatment significantly reduces p53 expression and upregulates sirtuin 1 (SIRT1) level in the lipopolysaccharide (LPS)-treated intestinal epithelial IEC6 cells. In addition, decreased nuclear translocation of nuclear factor-κB (NF-κB) and cell apoptosis were observed by miR-148a-3p mimic. Also, delivery of miR-148a-3p agomir in vivo exerts a similar protective role on NEC as BM^{EXO} treatment, accompanied by changes in p53 and SIRT1. Finally, the abolition of the protection of miR-148a-3p agomir on NEC was observed in a *Sirt1*-deficient ($Sirt1^{+/-}$) mouse. Collectively, our present study demonstrated that the miR-148a-3p/p53/SIRT1 axis has a considerable protective effect on NEC, and the agomir therapy provides a new treatment strategy for NEC.

KEY WORDS: Necrotizing enterocolitis; Human breast milk–derived exosomes; microRNA therapy; p53; Sirtuin 1

INTRODUCTION

Necrotizing enterocolitis (NEC) constitutes a gastrointestinal disease of premature infants that is characterized by the exaggerated inflammation and necrosis of the small intestine, resulting to overwhelming

[1]Department of Pediatrics, Shanghai Jiao Tong University Affiliated Sixth People's Hospital, No. 222 Huanhu West Third Road, Shanghai 201306, China
[2]To whom correspondence should be addressed at Department of Pediatrics, Shanghai Jiao Tong University Affiliated Sixth People's Hospital, No. 222 Huanhu West Third Road, Shanghai, 201306, China. Email: jialinzhang_2007@126.com

sepsis and death in many circumstances [1, 2]. The overall mortality rate (~30%) and morbidity, including long-term neuronal developmental disorders, remain high, especially in the setting of premature birth, formula feeding, and the bacterial colonization in gastrointestinal tract [3]. Therefore, it is a great urgency to understand its origins, and to investigate the novel prevention strategies for NEC. Of all the treatments, the breast milk delivery is reported to be the most effective [4, 5], and one of the leading protective roles could be associated with the highly enriched human breast milk–derived exosome (BM^{EXO}) [6]. Exosomes are extracellular vesicles between 30 and 150 nm in size that are released from multiple cell types, and are involved in the intercellular communication via fusing with target cell membranes or delivering the molecular cargo from parent cell to the recipient cell [7]. Previous study has revealed that the exosomes isolated from human breast milk improve the pro-proliferative and anti-apoptotic effects in stimulated intestinal epithelial cells, suggesting the protective properties of BM^{EXO} in NEC [8]. However, the complex content of BM^{EXO} and the technical challenges and costs required for the purification of pure BM^{EXO} are still major obstacles.

The internal cargos of exosomes are primarily microRNAs (miRNAs) and enzymes, and the former exerts most of the biological activities of exosomes [9]. miRNAs, which are 18–22 nucleotide non-coding RNAs, have been identified as a potential gene regulator via modulating gene expression post-transcriptionally. After entering the recipient cell, miRNAs form an RNA-induced silencing complex with the argonaute proteins and bind to the sequence of the 3′ untranslated region (3′ UTR) region of target mRNA(s) in a complementary manner to inhibit the protein translation [10, 11]. For example, other study has demonstrated that let-7d-5p could target galectin-3 and argonaute-2, thereby inhibiting the inflammatory response and intestinal epithelial cell apoptosis in the NEC rats [12]. However, which miRNA(s) in BM^{EXO} play a major role in the protection of NEC and the underlying mechanism are still poorly understood.

Therefore, the aims of the present study were (1) to confirm the protective effect of BM^{EXO} on NEC mice; (2) to identify the miRNA(s) enriched in BM^{EXO} and their downstream mechanisms; (3) to introduce a synthetic miRNA with higher stability and unity to replace the BM^{EXO} therapy.

METHODS

Animals

All experiments and procedures involving mice were carried out in accordance with the guide for the Care and Use of Laboratory Animals of the National Institutes of Health (NIH; Bethesda, MD, USA), and were approved by Animal Care and Use Committee of the Shanghai Jiao Tong University Affiliated Sixth People's Hospital. C57BL/6 mice at 8 weeks of age were obtained from the Experimental Animal Center of Shanghai Jiao Tong University Affiliated Sixth People's Hospital and housed in a constant-temperature room with a 12 h dark/12 h light circle and allowed free access to standard rodent chow and water. Intestinal epithelial-specific heterozygous *Sirt1*-knockout ($Sirt1^{+/-}$) mice and their wild-type littermates ($Sirt1^{+/+}$) on a C57BL/6 background were generated as previously described [13, 14].

Induction of NEC Models

NEC mice were induced in a well-validated method in 9-day-old mouse pups of either gender as previously described [15–17]. Briefly, the newborn mice were gavage fed (five times per day) with Similac Advance infant formula (Abbott Nutrition; Chicago, IL, USA) and Esbilac (PetAg; Hampshire, IL, USA) canine milk replacer with a ratio of 2:1, which was supplemented with enteric bacteria from a sample from an infant with surgical NEC. Pups were simultaneously subjected to hypoxic conditions (5% O_2 and 95% N_2) for 10 min in a hypoxia chamber (Billups-Rothenberg, San Diego, CA, USA) twice per day for 5 consecutive days. Age-matched breast milk–fed (BF) newborn mice were severed as healthy controls.

BMEXO Isolation

Human breast milk was obtained from the frozen stocks contributed by donors and was centrifuged twice at 3,000 g for 10 min at 25 °C. The fat layer was discarded and supernatant was moved to a new tube. After a third centrifugation at 5,000 g for 30 min at 25 °C, the supernatant was filtered with a 0.22 μm filter. Afterwards, a final ultracentrifugation at 32,000 g for 70 min at 4 °C was performed, and the pellet was resuspended in sterile

phosphate buffer saline (PBS). The nanoparticle tracking analysis was performed via a NanoSight NS300 system (Malvern Panalytical; Malvern, UK) to determine the particle size and particle concentration.

Animal Experiments

The experimental BM^{EXO} mice were intraperitoneally injected with 0.037 mg/μL BM^{EXO} in a 400 μL PBS solution once daily 1 h before the NEC induction for 5 consecutive days. The PBS mice were injected with an equal amount of sterile PBS solution. For miR-148a-3p agomir administration, 20–160 nmol miR-148a-3p agomir (Ribobio; Guangzhou, China) in a 400 μL PBS was injected once daily 1 h prior to each NEC procedure for 5 consecutive days. The treatment of negative control (NC) agomir was used as a control group. The weight and feed intake of each mouse were recorded. The collection of ileal tissue was performed at a fixed point in the terminal ileum 2 cm proximal to the cecum, which was also used to evaluate the NEC severity.

Cell Culture and Treatment

Small intestinal epithelial IEC6 cell line was purchased from American Type Culture Collection (ATCC; Manassas, VA, USA) and maintained in Dulbecco's Modified Eagle's Medium supplemented with 10% fetal bovine serum and 40 μg/L insulin (all from Gibco; Grand Island, NY, USA). Cells were treated with 100 ng/mL lipopolysaccharides (LPS; Beyotime, S1732; Shanghai, China) for 6 h, followed by 100 nM miR-148a-3p mimic or NC mimic (Ribobio) for 24 h before further use. IEC6-derived exosomes ($IEC6^{EXO}$) were isolated as described above.

Histological Analysis

The ileal tissues were sectioned at 8 μm and stained with Hematoxylin and Eosin Staining Kit (Beyotime, C0105) according to the manufacturer's instructions and observed under an optical microscope. For immunostaining, sections or cell slides were fixed in 4% paraformaldehyde, permeabilized in 0.25% triton X-100, and blocked in Ultra-V Block buffer for 10 min at room temperature, followed by the overnight incubation of primary antibodies [ZO-1 (Abcam, ab190085; Cambridge, UK), nuclear factor-κB (NF-κB; Abcam, ab32536), and GAPDH (Abcam, ab8245)] at 1:100 dilution at 4 °C, and the incubation of secondary antibodies for 2 h at room temperature. Nuclei were counterstained with DAPI (Beyotime, P0131). Fluorescence photos were taken by a FV3000 confocal microscope (Olympus; Tokyo, Japan). For TUNEL staining, cell slides were stained with a One Step TUNEL Apoptosis Assay Kit (Beyotime, C1088) in accordance with the manufacturer's protocols.

miRNA Sequencing

Total RNA was extracted via miRNeasy Mini kit (Qiagen, 217,004; Hilden, Germany), and small RNA libraries were generated via TruSeq Small RNA Library Preparation kit (Illumina, RS-200; San Diego, USA). All libraries were sequenced on an Illumina HiSeq3000 system to produce 50-bp paired end reads, which were demultiplexed via Casava v1.8.2. High-quality reads were obtained by trimming adapter sequences, invalid and low-quality reads from the raw reads. The sequences were adjusted via comparing the sequences in miRBase v22.1 [18], Rfam v14.5 [19], SILVA v138.1 [20], and Repbase v20.04 [21] databases, followed by the miRNA analysis via a miRDeep2 package. The correlation between $IEC6^{EXO}$ and BM^{EXO} samples was evaluated via Pearson's correlation coefficient, and the difference analysis of miRNA was performed via a edgeR [22] package.

Dual-Luciferase Reporter Assay

The 274–298 sequences in the 3′ UTR of *Tp53* were amplified in IEC6 or HEK293T cells and cloned into the region between the *XhoI* site to the *SalI* site of the pMIR-GLO expression plasmid (Promega, E1330; Madison, WI, USA). The site mutation of miR-148a-3p-targeted *Tp53* luciferase reporter vector was accomplished via a QuikChange II XL Site-Directed Mutagenesis Kit (Agilent, 200,521; Santa Clara, USA). The sequences of all plasmids were confirmed by DNA sequencing. Cells were transfected with miR-148a-3p mimic, NC mimic, miR-148a-3p inhibitor (Ribobio), NC inhibitor (Ribobio), *Tp53* pMIRGLO plasmid, or mutant *Tp53* pMIRGLO plasmid, and after 24 h, the ratio of Firefly luciferase/Renilla luciferase was detected.

Quantitative Reverse Transcription PCR (qRT-PCR)

RNA isolation was performed by a TRIzol reagent (Invitrogen, 15,596,018; Carlsbad, CA, USA), and the

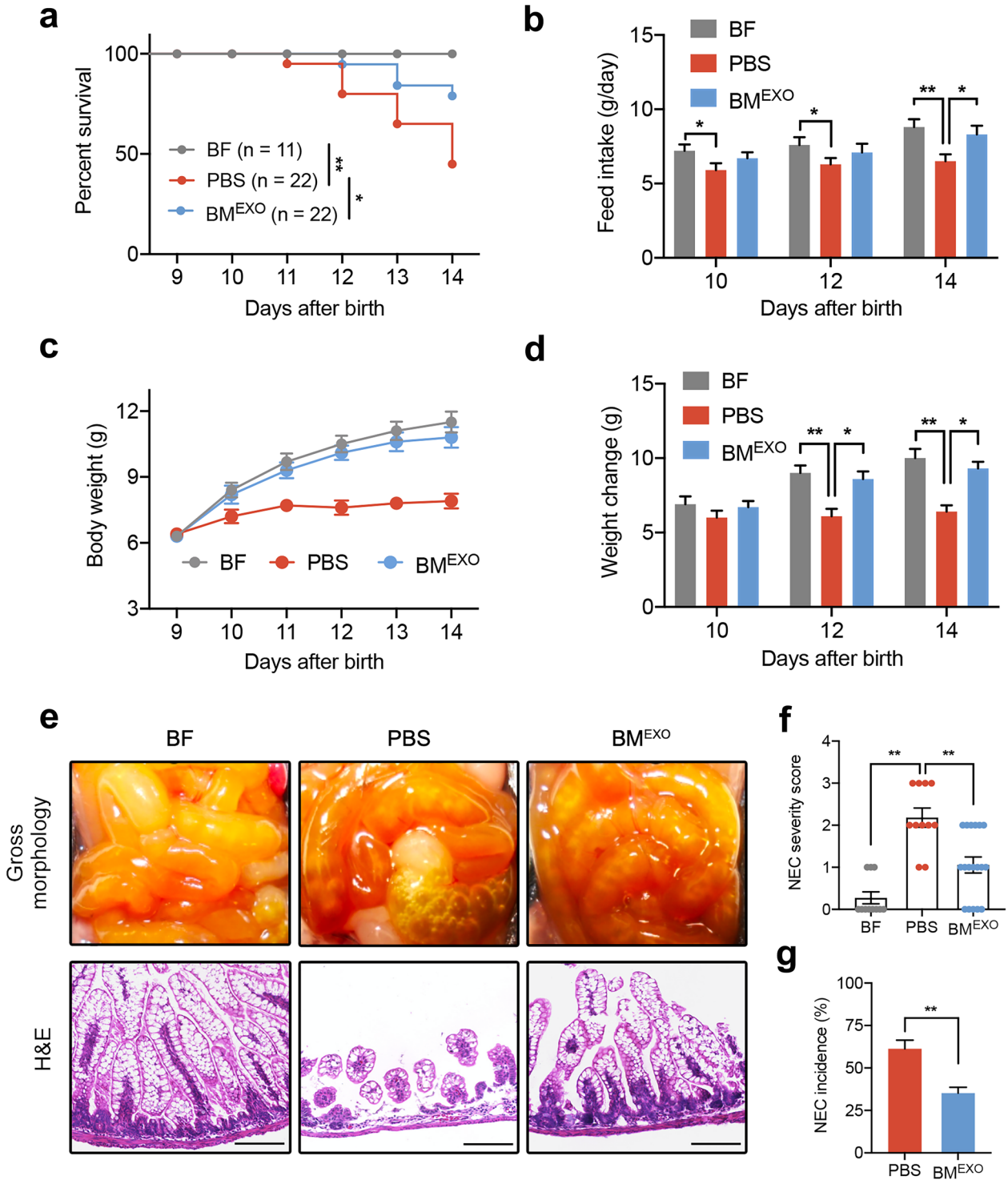
a
Percent survival
100
50
0
BF (n = 11)
PBS (n = 22)
BMEXO (n = 22)
**
*
9 10 11 12 13 14
Days after birth
b
Feed intake (g/day)
15
10
5
0
BF
PBS
BMEXO
*
*
**
*
10 12 14
Days after birth
c
Body weight (g)
12
9
6
3
BF
PBS
BMEXO
9 10 11 12 13 14
Days after birth
d
Weight change (g)
15
10
5
0
BF
PBS
BMEXO
**
*
**
*
10 12 14
Days after birth
e
BF
PBS
BMEXO
Gross morphology
H&E
f
NEC severity score
4
3
2
1
0
**
**
BF
PBS
BMEXO
g
NEC incidence (%)
100
75
50
25
0
**
PBS
BMEXO

◀ **Fig. 1** BM^{EXO} prevents NEC injury in the intestine of mice. (**a**) Kaplan–Meier curves and log-rank tests were used to investigate the survival rates of breastfed (BF) mouse pups and NEC pups with PBS or BM^{EXO} treatment. (**b**) Feed intake in BF, PBS, and BM^{EXO} pups on day 10, 12, and 14 after birth. (**c**, **d**) Body weight (**c**) and weight changes (**d**) in BF, PBS, and BM^{EXO} groups were recorded. (**e**) Representative gross images of small intestine (upper panel) and H&E-stained images of ileum (lower panel) in BF, PBS, and BM^{EXO} pups. Scale bars = 100 μm. (**f**) Quantitative analysis of NEC severity in BF ($n = 11$ mice), PBS ($n = 11$ mice), and BM^{EXO} ($n = 18$ mice) groups. (**g**) NEC incidence (score ≥ 2) in PBS ($n = 11$ mice) and BM^{EXO} ($n = 18$ mice) mouse pups. $^{*}p < 0.05$; $^{**}p < 0.01$.

RNA concentration was determined via a NanoDrop 2000c system (Thermo Fisher; Waltham, MA, USA). The cDNA libraries were constructed via the reverse transcription with SuperScript II Reverse Transcriptase (Thermo Fisher, 18,064), and the quantitative PCR was performed using the PowerTrack SYBR Green Master Mix (Applied Biosystems, A46109; Foster city, CA, USA). miRNAs were reverse transcripted with a TaqMan miRNA Reverse Transcription Kit (Applied Biosystems, 4,366,596), followed by the quantitation of miRNAs by TaqMan Advanced miRNA Assays (Applied Biosystems, A25576). The expression of mRNA was normalized to *Gapdh* via the standard $2^{-\Delta\Delta Ct}$ method. The primer sequences were *Tnf-α* (Forward: 5′-CCCTCACACTCA GATCATCTTCT-3′; Reverse: 5′-GCTACGACGTGG GCTACAG-3′), *Il6* (Forward: 5′-TCTATACCACTT CACAAGTCGGA-3′; Reverse: 5′-GAATTGCCATTG CACAACTCTTT-3′), *Egf* (Forward: 5′-TTAACGGGA CAGGACTAGAGAAA-3′; Reverse: 5′-AAGGAACTT AGAAGAACTCGGGA-3′), *Il10* (Forward: 5′-GCTGGA CAACATACTGCTAACC-3′; Reverse: 5′-ATTTCCGAT AAGGCTTGGCAA-3′), *Tp53* (Forward: 5′-CTCTCC CCCGCAAAAGAAAAA-3′; Reverse: 5′-CGGAAC ATCTCGAAGCGTTTA-3′), *Sirt1* (Forward: 5′-GCT GACGACTTCGACGACG-3′; Reverse: 5′-TCGGTCAAC AGGAGGTTGTCT-3′), and *Gapdh* (Forward: 5′-AGG TCGGTGTGAACGGATTTG-3′; Reverse: 5′-TGTAGA CCATGTAGTTGAGGTCA-3′).

Western Blot Analysis

The proteins of ileal tissue and IEC6 cells were extracted via RIPA lysis buffer (Beyotime, P0013) and separated through gel electrophoresis. After transferring onto polyvinylidene difluoride membranes (Millipore, IPVH00010; Burlington, MA, USA), the membranes were blocked in 5% skimmed milk for 2 h, and then incubated overnight with primary antibodies (acetylated-p53 (Abcam, ab183544), p53 (Abcam, ab26), SIRT1 (Cell Signaling, 8469; Boston, MA, USA), ZO-1, NF-κB, Alix (ab275377), CD9 (ab92726), CD63 (ab216130), TSG101 (ab133586), and GAPDH) at 1:1000 dilution at 4 °C. Finally, the membranes loaded with protein ladders were incubated with HRP-conjugated secondary antibodies for 2 h at room temperature and exposed via enhanced chemiluminescence.

Statistical Analysis

Data were shown as means ± standard error of mean (SEM). Differences between two groups were performed by Student's *t* test, and multiple comparisons were analyzed by one-way analysis of variance (ANOVA) followed by Tukey's post hoc test. Survival analysis was evaluated via a Kaplan–Meier survival curve and log-rank statistics test. Statistical analyses were carried out through a Prism 8 software (GraphPad; San Diego, CA, USA), and $p < 0.05$ was considered statistically significant.

RESULTS

BMEXO Decreases the Level of NEC Severity in Mouse Pups

To investigate the protective role of BM^{EXO} on NEC, exosomes were isolated from human breast milk and identified (Fig. S1), and then injected into the well-established models of NEC. As shown in Fig. 1a, the NEC mouse pups showed a significant increase in mortality compared to BF pups, which was reversed by the administration of BM^{EXO} during the establishment of the NEC model. In addition, the poor feed intake and weight gain in response to NEC were significantly improved in the BM^{EXO} groups (Fig. 1b–d). The small intestine of NEC mice showed extensive edema, thickening, and air within the bowel wall (also called *pneumatosis intestinalis*, a hallmark symptom of human NEC), whereas the intestine of BF control mice revealed healthy appearing (Fig. 1e). Consistently, histological examination of the intestine of NEC mice showed extensive villous sloughing, separation of submucosa, and edema in the submucosal and muscular layers (Fig. 1e). Delivery of BM^{EXO} significantly protected against NEC process, as evidenced by gross appearance of the intestine, intestinal histology (Fig. 1e), and NEC severity (Fig. 1f). The incidence rate of NEC was also significantly reduced in the BM^{EXO} group (Fig. 1g).

The BMEXO Effect on Anti-inflammation and Strengthening of Tight Junctions of NEC Intestine

We next determine the relationship between BM^{EXO} treatment and the regulation of either pro-inflammatory or anti-inflammatory cytokines. The qRT-PCR analysis was performed to measure the mRNA expression of helper T-cell 1 (TH1) cytokine (tumor necrosis factor (TNF-α)), interleukin-6 (IL-6), epidermal growth factor (EGF), and helper T-cell 2 (TH2) cytokine (IL-10), and the results demonstrated that NEC induced a significant increase in mRNA expression of pro-inflammatory factors (TNF-α and IL-6), which was prevented by the BM^{EXO} administration (Fig. 2a, b). Conversely, the downregulated mRNA

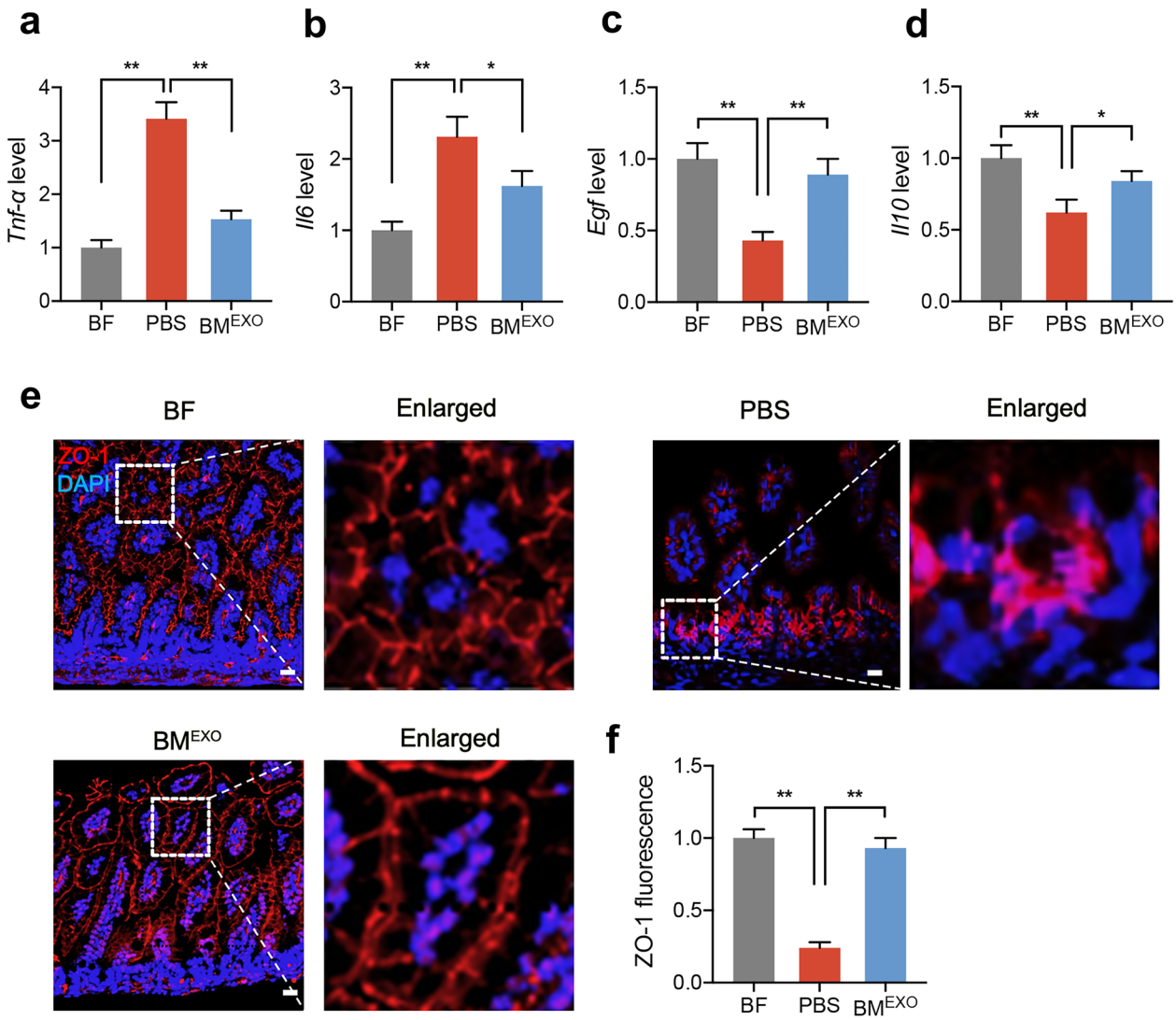

Fig. 2 BM^{EXO} decreases intestinal inflammation and improves tight junctions in NEC mouse pups. (**a**, **b**) qRT-PCR analysis was used to determine the mRNA expression of pro-inflammatory factors such as *Tnf-α* (**a**) and *Il6* (**b**) in the ileum of mouse pups, $n=4$ independent experiments per group. (**c**, **d**) mRNA levels of anti-inflammatory factors including *Egf* (**c**) and *Il10* (**d**) in the ileum tissues, $n=4$ independent experiments per group. (**e**) Representative ZO-1 staining in the ileum of mouse pups. Scale bars = 25 μm. (**f**) Quantitation of fluorescence intensity of ZO-1 in BF, PBS, and BM^{EXO} groups, $n=5$ independent experiments per group. $^{*}p<0.05$; $^{**}p<0.01$.

expression of anti-inflammatory factors in the NEC intestine was significantly reversed by BM^{EXO} (Fig. 2c, d). Importantly, inactivation EGF receptor in animals results in intestinal lesions resembling NEC, and breastfeeding with EGF supplement can reduce the incidence of NEC and the level of disease severity [23]. In line with the pervious study, we observed a significant recovery of *Egf* expression in the intestinal tissues of NEC mice after BM^{EXO} treatment (Fig. 2c).

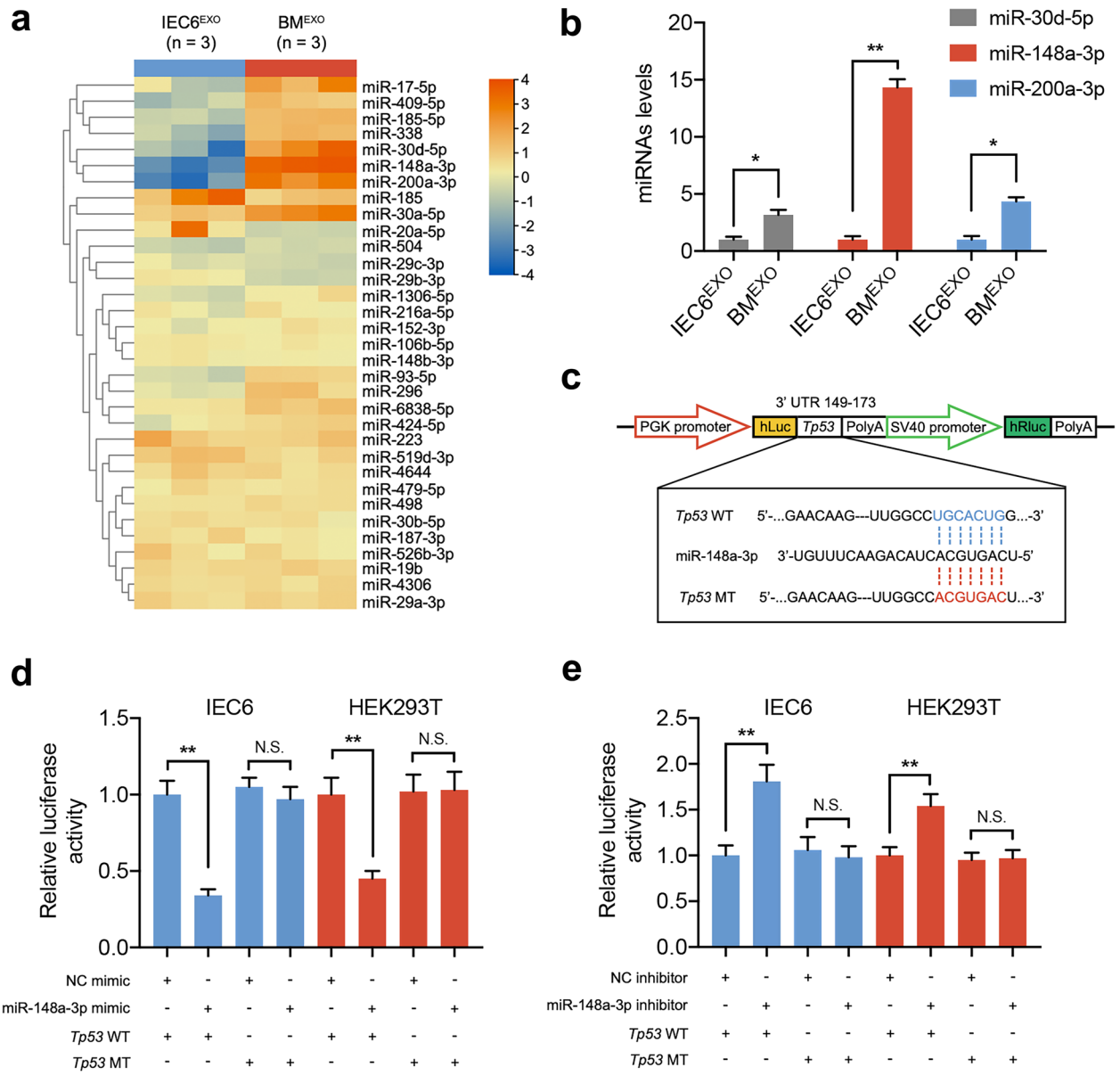

Fig. 3 BM^{EXO}-enriched miR-148a-3p directly targets *Tp53*. (**a**) miRNA sequencing in IEC6 cell–derived exosomes ($IEC6^{EXO}$) and BM^{EXO}, and the heatmap showed the most enriched miRNAs in BM^{EXO}. (**b**) miR-30d-5p, miR-148a-3p, and miR-200a-3p levels were determined through qRT-PCR in $IEC6^{EXO}$ and BM^{EXO}, $n=4$ independent experiments per group. (**c**) The predicted miR-148a-3p binding sites in the 3′ UTR of *Tp53* and the construction of wild-type (WT) and mutant (MT) dual-luciferase reporter plasmids. (**d**, **e**) Relative luciferase activity assays were performed in IEC6 or HEK293T cell lines transfected with miR-148a-3p mimic (**d**) or miR-148a-3p inhibitor (**e**) and *Tp53* WT or *Tp53* MT, $n=3$ independent experiments per group. $^{*}p<0.05$; $^{**}p<0.01$; N.S.: not significant.

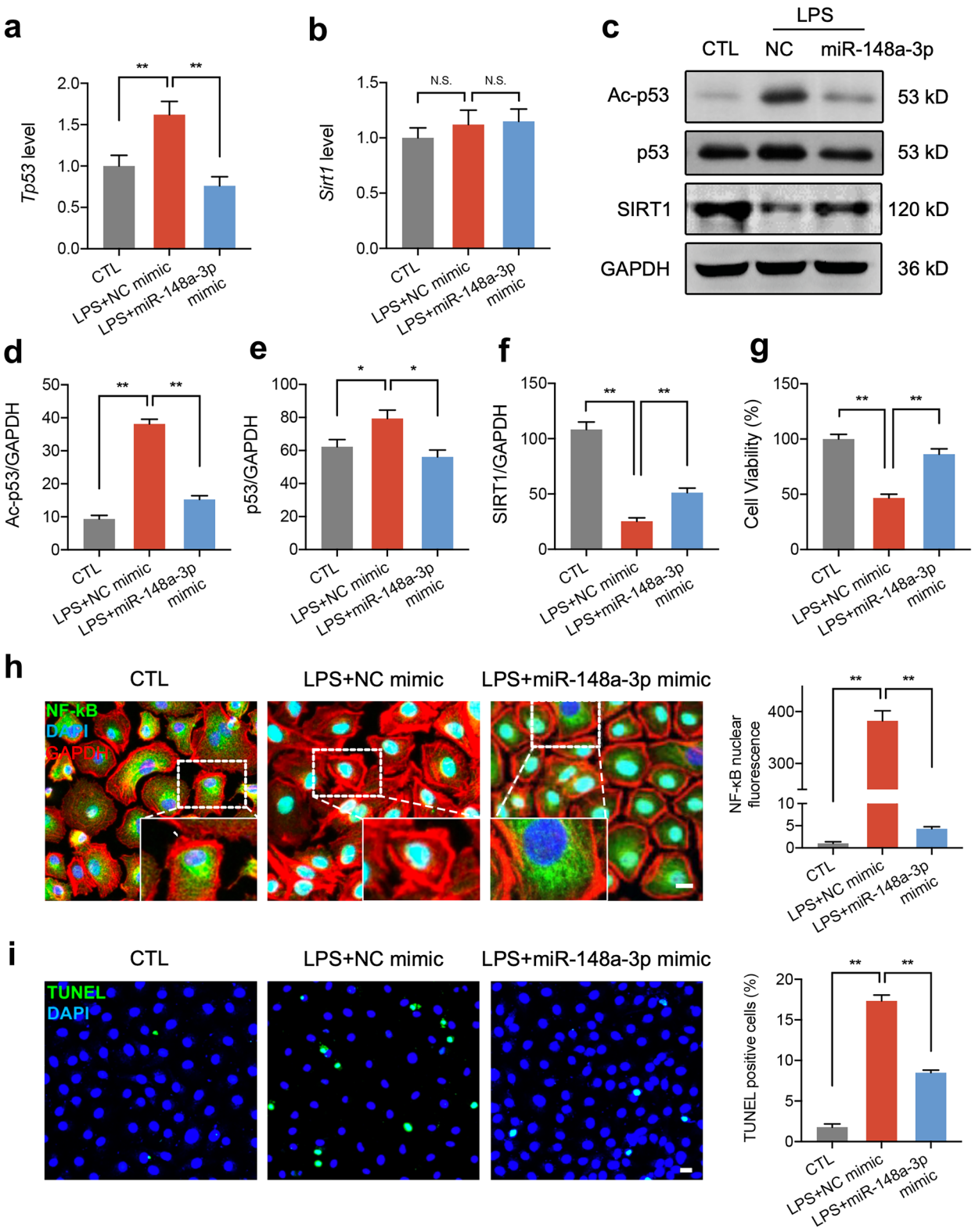
a
Tp53 level
2.0
1.5
1.0
0.5
0.0
**
**
CTL
LPS+NC mimic
LPS+miR-148a-3p mimic
b
Sirt1 level
1.5
1.0
0.5
0.0
N.S.
N.S.
CTL
LPS+NC mimic
LPS+miR-148a-3p mimic
c
LPS
CTL
NC
miR-148a-3p
Ac-p53
p53
SIRT1
GAPDH
53 kD
53 kD
120 kD
36 kD
d
Ac-p53/GAPDH
50
40
30
20
10
0
**
**
CTL
LPS+NC mimic
LPS+miR-148a-3p mimic
e
p53/GAPDH
100
80
60
40
20
0
*
*
CTL
LPS+NC mimic
LPS+miR-148a-3p mimic
f
SIRT1/GAPDH
150
100
50
0
**
**
CTL
LPS+NC mimic
LPS+miR-148a-3p mimic
g
Cell Viability (%)
150
100
50
0
**
**
CTL
LPS+NC mimic
LPS+miR-148a-3p mimic
h
CTL
LPS+NC mimic
LPS+miR-148a-3p mimic
NF-kB
DAPI
GAPDH
NF-κB nuclear fluorescence
400
300
10
5
0
**
**
CTL
LPS+NC mimic
LPS+miR-148a-3p mimic
i
CTL
LPS+NC mimic
LPS+miR-148a-3p mimic
TUNEL
DAPI
TUNEL positive cells (%)
20
15
10
5
0
**
**
CTL
LPS+NC mimic
LPS+miR-148a-3p mimic

◀ **Fig. 4** miR-148a-3p upregulates SIRT1 expression and decreases cell injury in LPS-treated IEC6 cells. (**a**, **b**) mRNA expression of *Tp53* (**a**) and *Sirt1* (**b**) was investigated in control (CTL), LPS + negative control (NC) mimic– or miR-148a-3p mimic–treated IEC6 cells, $n = 4$ independent experiments per group. (**c**–**f**) Representative immunoblots of acetylated (Ac)-p53, p53, SIRT1, and GAPDH (**c**) and quantitative analysis of Ac-p53/GAPDH (**d**), p53/GAPDH (**e**), and SIRT1/GAPDH (**f**) in IEC6 cells, $n = 3$ independent experiments per group. (**g**) Cell viability of IEC6 cells was determined by CCK-8 assays, $n = 5$ independent experiments per group. (**h**) Representative NF-κB staining and quantitation of nuclear fluorescence intensity of NF-κB in IEC6 cells (enlarged images were shown below), $n = 4$ independent experiments per group. Scale bars = 25 μm. (**i**) Representative TUNEL staining and quantitation of TUNEL positive IEC6 cells, $n = 4$ independent experiments per group. Scale bars = 25 μm. $^{*}p < 0.05$; $^{**}p < 0.01$; N.S.: not significant.

The distribution and expression of the tight junction protein ZO-1 was then investigated. As shown in Fig. 2e, the continuity of ZO-1 was interrupted in the NEC newborn ileum, accompanied by a significant increase in ZO-1 endocytosis, and BM^{EXO} treatment can significantly restore the linearity of ZO-1. Furthermore, the declined ZO-1 expression in NEC mice was also prevented by the administration of BM^{EXO} (Fig. 2f).

miR-148a-3p Binds Directly to Tp53

As miRNAs are important biologically active loads in BM^{EXO} [6], we compared the difference in miRNA abundance in small intestinal epithelial IEC6 cell–derived exosomes ($IEC6^{EXO}$) and BM^{EXO} through miRNA sequencing, and the results revealed that 3 miRNAs including miR-30d-5p, miR-148a-3p, and miR-200a-3p are the most abundant in BM^{EXO} (Fig. 3a). Among them, miR-148a-3p was identified as the miRNA that show greater expression in BM^{EXO} than in $IEC6^{EXO}$ (Fig. 3b). Subsequently, we predicted that the downstream target gene of miR-148a-3p may be *Tp53* through an online TargetScan databases (Fig. 3c), as the downregulation of its encoded protein expression is beneficial to the intestinal recovery of NEC [24]. To further determine whether miR-148a-3p directly target *Tp53*, a dual-luciferase reporter assay was performed via a luciferase expression vector containing the *Tp53* fragment with the presumptive miR-148a-3p binding sites (Fig. 3c). As shown in Fig. 3d, miR-148a-3p mimic treatment significantly decreased the activity of luciferase expression vector carrying the *Tp53* wild-type (WT) sequence both in IEC6 and HEK293T cells, and the mutation (MT) of these binding sites reversed the inhibitory role of miR-148a-3p mimic (Fig. 3d). In contrast, miR-148a-3p inhibitor significantly enhanced the luciferase activity, whereas the administration of MT vector abolished this effect (Fig. 3e). Collectively, these results suggested that miR-148a-3p can directly act on *Tp53*.

miR-148a-3p Prevents IEC6 Cells from LPS-Mediated Cell Injury

Given that the BM^{EXO}-enriched miR-148a-3p targets *Tp53*, we then evaluated the protective role of miR-148a-3p on the lipopolysaccharide (LPS)-treated IEC6 cells and the downstream mechanism. As an anti-inflammatory protein, sirtuin 1 (SIRT1) has been reported to suppress nuclear factor-κB (NF-κB) acetylation and nuclear translocation [25], and is predominantly linked to p53 activity [26]. We observed that miR-148a-3p mimic significantly increased the *Tp53* expression but not *Sirt1* in the LPS-stimulated IEC6 cells (Fig. 4a, b). Furthermore, western blot analysis demonstrated that in addition to reducing the acetylated p53 and total p53 levels, miR-148a-3p mimic treatment also restored the decreased SIRT1 protein expression in the LPS-treated IEC6 cells (Fig. 4c–f). Additionally, miR-148a-3p mimic treatment resulted in a significant increase in cell viability and a reduction in the nuclear translocation of NF-κB (Fig. 4g, h). In conclusion, these results revealed that miR-148a-3p decreases the LPS-induced cell injury via the regulation of p53 and SIRT1 in vitro.

miR-148a-3p Agomir Exerts a Protective Effect Similar to that of BMEXO in NEC Mice

To testify whether the single use of miR-148a-3p also protects the intestines of NEC mice, we injected miR-148a-3p agomir (2′OMe + 5′chol modified to increase the transfection efficiency in tissues) into NEC mice with different concentration gradients, and the results showed that a daily dose of 80 nmol agomir can maintain a stable high level of miR-148a-3p in mice (Fig. 5a). In addition, administration of miR-148a-3p agomir with 80 nmol/day displayed similar NEC protection to BM^{EXO} in gross appearance of the intestine, intestinal histology (Fig. 5b), NEC severity (Fig. 5c), and NEC incidence (Fig. 5d). Congruously, miR-148a-3p agomir also downregulated the mRNA expression of pro-inflammatory factors (Fig. 5e, f) and promoted the mRNA levels of anti-inflammatory factors (Fig. 5g, h).

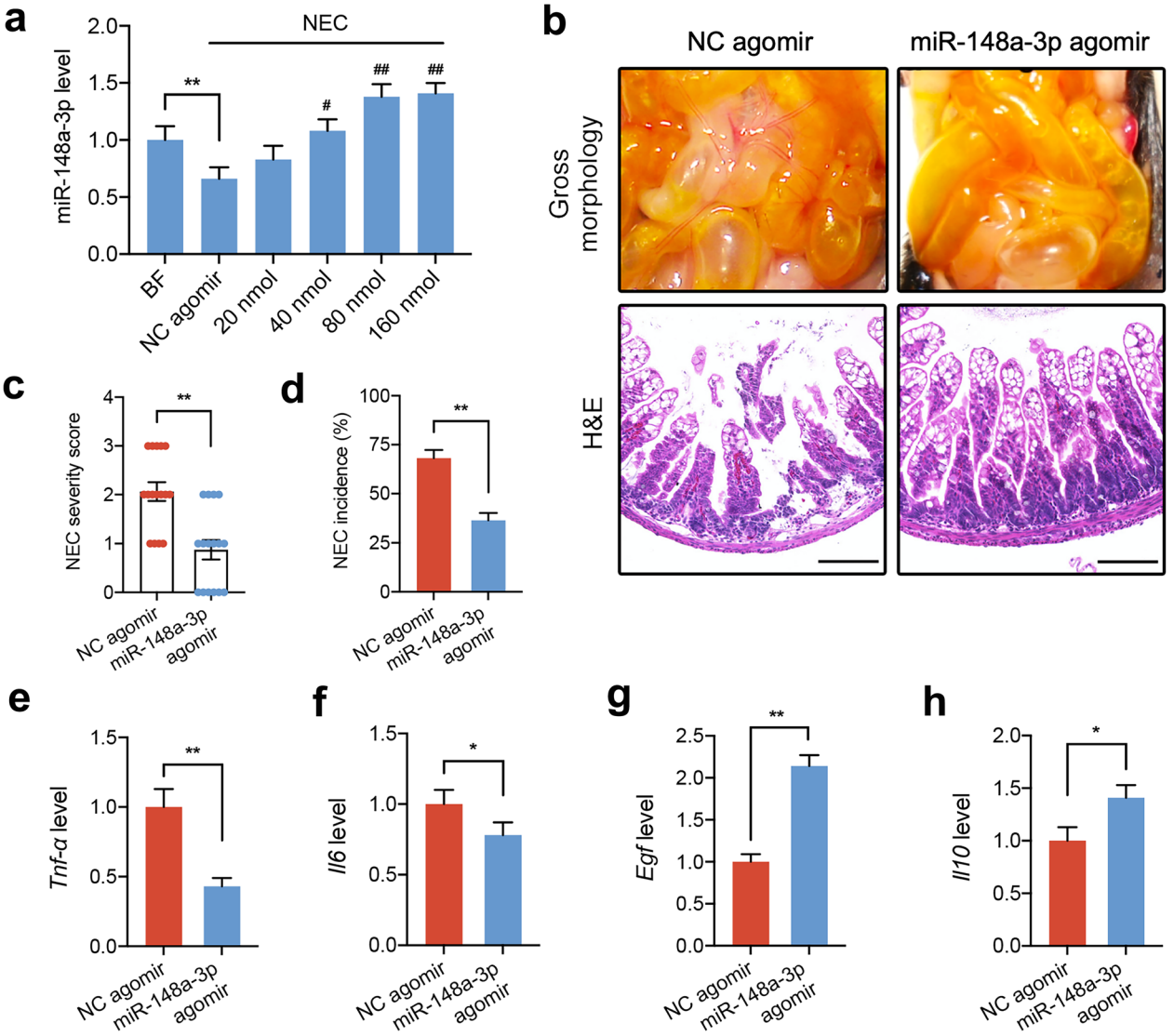

Fig. 5 miR-148a-3p agomir attenuates intestinal NEC damage consistent with the therapeutic effect of BM^{EXO}. (**a**) miR-148a-3p level in the ileum tissues of BF, NEC + NC agomir, and NEC + miR-148a-3p agomir (20 nmol to 160 nmol) mouse pups, $n = 3$ independent experiments per group. (**b**) Representative gross images of small intestine (upper panel) and H&E-stained images of ileum (lower panel) in NEC + NC agomir and NEC + miR-148a-3p agomir pups. Scale bars = 100 μm. (**c**) Quantitative analysis of NEC severity in NEC + NC agomir ($n = 16$ mice) and NEC + miR-148a-3p agomir ($n = 16$ mice) groups. (**d**) NEC incidence in NEC + NC agomir and NEC + miR-148a-3p agomir mouse pups. (**e** and **f**) mRNA expression of pro-inflammatory factors including *Tnf-α* (**e**) and *Il6* (**f**) in the ileum of mouse pups, $n = 4$ independent experiments per group. (**g**, **h**) mRNA levels of anti-inflammatory factors such as *Egf* (**g**) and *Il10* (**h**) in the ileum tissues, $n = 4$ independent experiments per group. $^{*}p < 0.05$; $^{**}p < 0.01$; $^{\#}p < 0.05$, $^{\#\#}p < 0.01$ vs. NC agomir group.

Blocking the SIRT1 Pathway Decreases the Beneficial Role of miR-148a-3p Agomir in NEC MiceIn Vivo

The role of miR-148a-3p/*Tp53*/*Sirt1* axis was then verified in NEC mice because it was found to be involved in the protective effect of miR-148a-3p in the LPS-stimulated ICE6 cells. As shown in Fig. 6a, b, miR-148a-3p agomir treatment reduced the *Tp53* level, but there was no significant difference in *Sirt1* expression between miR-148a-3p agomir group and control group. Furthermore, the application of agomir decreased the Ac-p53, p53, and NF-κB expression and upregulated the ZO-1 level as well as SIRT1 (Fig. 6c). Correlation analysis showed that the SIRT1 level was significantly negatively correlated with the expression of Ac-p53 and p53, indicating that SIRT1 may be a downstream target of p53 (Fig. 6d, e). To confirm this, the intestinal epithelial-specific heterozygous *Sirt1*-knockout (*Sirt1*$^{+/-}$) mice were used. As shown in Fig. 6f, *Sirt1* deficiency abolished the improvement of NEC intestinal histology by miR-148a-3p agomir, and the increased NEC severity and incidence were also observed in the miR-148a-3p agomir–treated *Sirt1*$^{+/-}$ mice (Fig. 6g, h). Additionally, the miR-148a-3p agomir–induced downregulation of pro-inflammatory cytokines and upregulation of anti-inflammatory cytokines were all reversed by *Sirt1* depletion (Fig. 6i–l). Taken together, these findings demonstrated that the miR-148a-3p/*Tp53*/*Sirt1* axis may serve as a therapeutic target for NEC.

DISCUSSION

It is well-established that BM^{EXO} has the ability to potentially influence the immune system of the newborn infant. The exosomes from breast milk safely transfer the miRNAs from mother to baby and improve the proliferation of intestinal epithelial cells in NEC in preterm infants [27, 28]. In addition, BM^{EXO} also regulates the absorptive epithelial cell renewal and viability in the intestine of infant [29]. However, it is not clear which miRNA(s) play a major role in the protection of NEC and the downstream mechanisms. In the present study, our findings demonstrated that the treatment of BM^{EXO} significantly improves the survival rate of NEC neonatal mice and reduces the intestinal injury and inflammation. Furthermore, as one of the most enriched miRNAs in BM^{EXO}, miR-148a-3p directly targets *Tp53* and decreases the LPS-stimulated IEC6 cell apoptosis and NF-κB nuclear translocation. Finally, the modified miR-148a-3p agomir can reproduce all the protective effects of BM^{EXO} on NEC, and its mechanism is related to the participation of p53 and SIRT1.

NEC is a multifactorial gastrointestinal disease that occurs in response to multiple risk factors such as premature birth, enteral feeding, alteration in enteric mucosal integrity, and the presence of pathogenic microorganisms, and results in the serious intestinal inflammatory response and injury. Moreover, the activation of lipopolysaccharide receptor toll-like receptor 4 (TLR4) in the NEC intestines was more pronounced when compared to the intestines of full-term infants, leading to an intestinal mucosa disruption, bacterial translocation into the blood circulation [30–32]. The activation of TLR4 on the endothelial cells simultaneously causes vasoconstriction and intestinal ischemia, which characterizes NEC [33]. In line with the pervious study by others [8], we demonstrated that BM^{EXO} administration dramatically improves the pathological changes in the intestines of NEC mice, and reduces the NEC score and incidence. Additionally, BM^{EXO} also reduces intestinal inflammation and restores tight junctions between intestinal epithelial cells in the NEC mice. However, in addition to the exosomes from breast milk, the human milk oligosaccharides (HMOs), such as disialyllacto-N-tetraose (DSNLT) [34] and 2′-fucosyllactose (2'FL) [35], are also reported to be responsible for the protective role of breast milk, indicating that breast milk is pleiotropic and it exerts a protective effect against NEC through a variety of internal substances. However, due to the complex and variable composition of the contents of breast milk, it is more beneficial to clinical translation of NEC treatment to identify an agent with the most therapeutic effect among the components of breast milk.

Since an extensive miRNA profiling of BM^{EXO} has been carried out in human [36, 37], cow [38], pig [39, 40], and panda [41], the results suggest that the abundantly present miRNAs are conserved between mammals. In this study, our miRNA sequencing analysis reveals that there are three miRNAs with the highest expression levels in BM^{EXO}, including miR-30d-5p, miR-148a-3p, and miR-200a-3p, which are consistent with previous studies [36]. Furthermore, we observed that the highest level of miRNAs in BM^{EXO} is miR-148a-3p, which directly binds to *Tp53* in both IEC6 and HEK293T cells and significantly inhibits the level of its encoded protein expression and acetylation modification. As expect, the

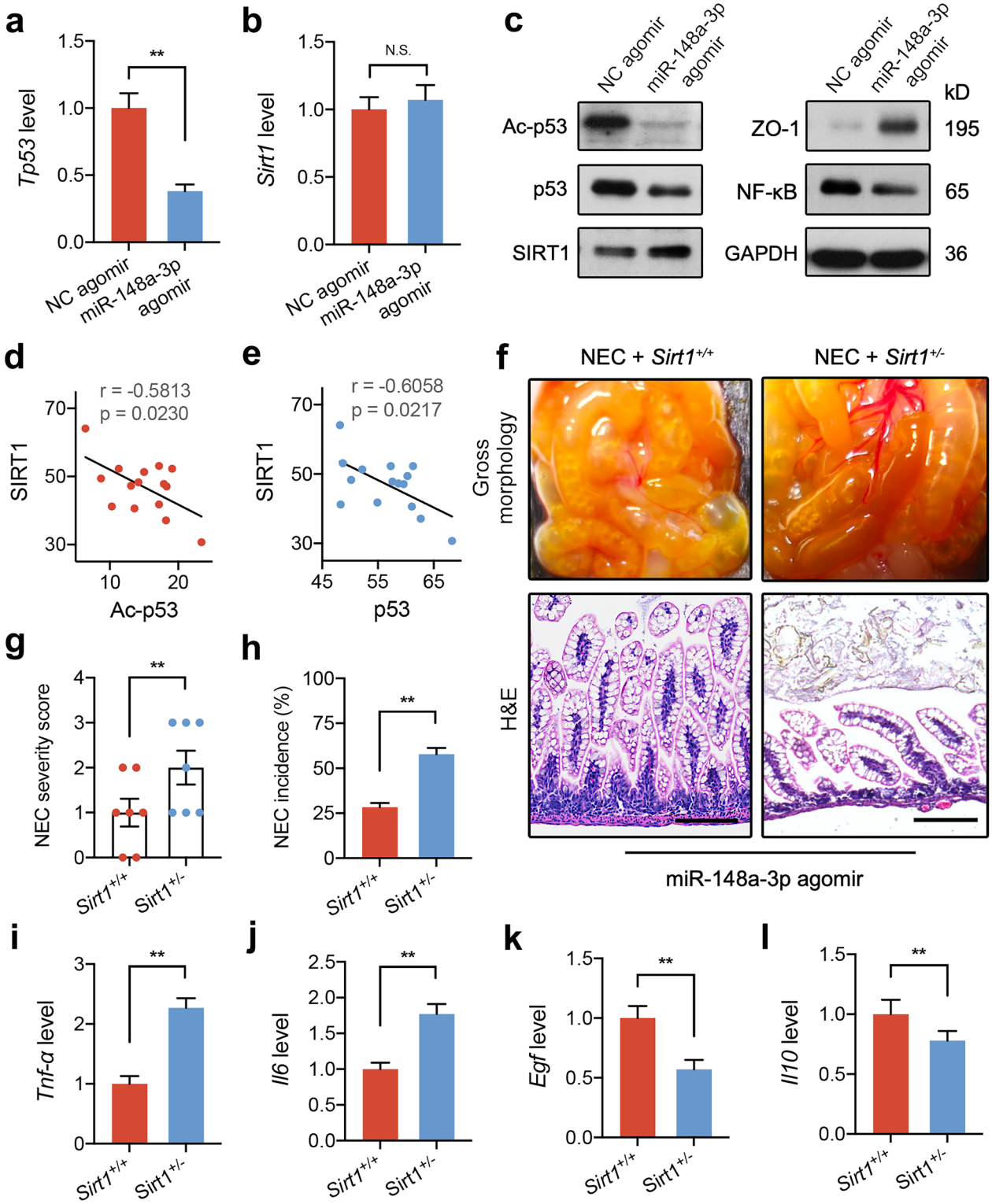
a
Tp53 level
1.5
1.0
0.5
0.0
**
NC agomir
miR-148a-3p agomir
b
Sirt1 level
N.S.
c
NC agomir
miR-148a-3p agomir
kD
Ac-p53
p53
SIRT1
ZO-1
NF-κB
GAPDH
195
65
36
d
r = -0.5813
p = 0.0230
SIRT1
Ac-p53
e
r = -0.6058
p = 0.0217
p53
f
NEC + Sirt1+/+
NEC + Sirt1+/-
Gross morphology
H&E
miR-148a-3p agomir
g
NEC severity score
h
NEC incidence (%)
i
Tnf-α level
j
Il6 level
k
Egf level
l
Il10 level
Sirt1+/+
Sirt1+/-

◀ **Fig. 6** The p53/SIRT1 axis is involved in the therapeutic effect of miR-148a-3p agomir on NEC. (**a**, **b**) mRNA levels of *Tp53* (**a**) and *Sirt1* (**b**) were determined in NEC + NC agomir and NEC + miR-148a-3p agomir pups, $n = 4$ independent experiments per group. (**c**) Representative immunoblots of Ac-p53, p53, SIRT1, ZO-1, NF-κB, and GAPDH. (**d**, **e**) Correlation analysis between Ac-p53 and SIRT1 expression (**d**) and p53 and SIRT1 expression (**e**), $n = 15$ independent experiments per group. (**f**) Representative gross images of small intestine (upper panel) and H&E-stained images of ileum (lower panel) in NEC wild-type ($Sirt1^{+/+}$) and intestinal epithelial-specific *Sirt1*-knockout ($Sirt1^{+/-}$) NEC mouse pups injected with miR-148a-3p agomir. Scale bars = 100 μm. (**g**) Quantitative analysis of NEC severity in miR-148a-3p agomir–treated $Sirt1^{+/+}$ ($n = 7$ mice) and $Sirt1^{+/-}$ ($n = 7$ mice) groups. (**h**) NEC incidence in $Sirt1^{+/+}$ and $Sirt1^{+/-}$ mouse pups. (**i**, **j**) Relative mRNA expression of pro-inflammatory factors including *Tnf-α* (**i**) and *Il6* (**j**) in the ileum of mouse pups, $n = 4$ independent experiments per group. (**k**, **l**) mRNA levels of anti-inflammatory factors such as *Egf* (**k**) and *Il10* (**l**) in the ileum tissues, $n = 4$ independent experiments per group. $^{**}p < 0.01$; N.S.: not significant.

treatment of miR-148a-3p mimic significantly reduces the NF-κB nuclear translocation and cell apoptosis in LPS-treated IEC6 cells, suggesting that miR-148a-3p may be the most important effector in BM^{EXO} for NEC protection.

Considering the technical challenges, costs, and complexity of content, it is difficult to obtain large quantities of pure and specific exosomes from a mixtures of different vesicle types. Furthermore, the uncontrolled exchange of genetic information between cell populations was also reported [42], indicating that the treatment of exosomes may cause unpredictable side effects. Therefore, a new and more specific treatment is needed. In this study, we delivered a modified miR-148a-3p agomir (2′OMe + 5′chol modified) into NEC mice to increase the transfection efficiency and stability in the intestines. The results revealed that the administration of 80 nmol miR-148a-3p agomir significantly decreases the intestinal pathological changes, NEC severity, and the inflammation intensity, consistent with the protective effect of BM^{EXO}. We also observed a significant decrease in Ac-p53, p53, and NF-κB expression and a significant promotion of SIRT1 and ZO-1 expression in the miR-148a-3p agomir–treated NEC mice. SIRT1 is an anti-inflammatory factor that has been reported to be associated with the regulation of NEC pathological process and p53 activity [13, 26]. Correlation analysis showed that the expression of SIRT1 is significantly negatively correlated with the levels of Ac-p53 and p53, suggesting that SIRT1 may be involved in the protection of miR-148a-3p/p53 pathway. We finally introduced the intestinal epithelial-specific heterozygous *Sirt1*-knockout ($Sirt1^{+/-}$) mice, and the results suggested that *Sirt1* deficiency makes the NEC mouse intestines lose their reactivity to miR-148a-3p agomir, further confirming the importance of SIRT1 in the downstream pathway of miR-148-3p.

This study also contains some limitations. For example, the protective effect and mechanism of miR-148a-3p have not been verified in large animals with more clinical translational significance or in the intestinal tissues of clinic NEC patients. Furthermore, there are a variety of enriched miRNAs in BM^{EXO} in addition to miR-148a-3p, such as miR-30d-5p, miR-200a-3p, miR-200c-3p, and let-7a-5p [36]. This may have better protection or prevention of NEC if a mixture of miRNA agomirs with different effects could injected simultaneously into NEC animals. Since we did not pay attention to gender when selecting mouse pups into the group, our study did not observe the difference in the efficacy of BMEXO and miR-148a-3p between NEC mice of different genders. Importantly, it is reported that BMEXO has an effective protective effect on the small intestine of LPS-induced male neonatal Kunming mice [43]. In addition, our results also reveal that BMEXO and miR-148a-3p agomir seem to have similar protective effects on male and female mice, as we recruited both male and female neonatal mice. However, whether gender plays a role in it needs to be further explored.

CONCLUSION

Taken together, our study investigated the protection of miR-148a-3p, one of the most enriched miRNAs in BM^{EXO}, on NEC by regulating p53 and SIRT1. In addition, we also confirmed that the use of miR-148a-3p agomir in vivo has a similar protective effect as BM^{EXO}, which provides a new idea for future treatment strategies for NEC.

SUPPLEMENTARY INFORMATION

The online version contains supplementary material available at https://doi.org/10.1007/s10753-021-01618-5.

AUTHOR CONTRIBUTION

Study design and experimentation: M. G., K. Z., and J. Z.; supervision: J. Z.; and manuscript writing: M. G. and J. Z.

DATA AVAILABILITY

The data used to support the findings of this study are included in the article.

DECLARATIONS

Ethics Approval and Consent to Participate All experiments and procedures involving mice were carried out in accordance with the guide for the Care and Use of Laboratory Animals of the NIH, and were approved by Animal Care and Use Committee of the Shanghai Jiao Tong University Affiliated Sixth People's Hospital.

Consent for Publication Not applicable.

Competing Interests The authors declare no competing interests.

REFERENCES

1. Kim, W., and J.M. Seo. 2020. Necrotizing enterocolitis. *New England Journal of Medicine* 383 (25): 2461.
2. Mara, M.A., M. Good, and J.H. Weitkamp. 2018. Innate and adaptive immunity in necrotizing enterocolitis. *Seminars in Fetal and Neonatal Medicine* 23 (6): 394–399.
3. Flahive, C., A. Schlegel, and E.A. Mezoff. 2020. Necrotizing enterocolitis: Updates on morbidity and mortality outcomes. *Journal of Pediatrics* 220: 7–9.
4. Schanler, R.J., R.J. Shulman, and C. Lau. 1999. Feeding strategies for premature infants: Beneficial outcomes of feeding fortified human milk versus preterm formula. *Pediatrics* 103 (6 Pt 1): 1150–1157.
5. Newburg, D.S., and W.A. Walker. 2007. Protection of the neonate by the innate immune system of developing gut and of human milk. *Pediatric Research* 61 (1): 2–8.
6. Galley, J.D., Besner, G.E. 2020. The therapeutic potential of breast milk-derived extracellular vesicles. *Nutrients* 12 (3).
7. Montecalvo, A., A.T. Larregina, W.J. Shufesky, D.B. Stolz, M.L. Sullivan, J.M. Karlsson, C.J. Baty, G.A. Gibson, G. Erdos, Z. Wang, et al. 2012. Mechanism of transfer of functional microRNAs between mouse dendritic cells via exosomes. *Blood* 119 (3): 756–766.
8. Pisano, C., J. Galley, M. Elbahrawy, Y. Wang, A. Farrell, D. Brigstock, and G.E. Besner. 2020. Human breast milk-derived extracellular vesicles in the protection against experimental necrotizing enterocolitis. *Journal of Pediatric Surgery* 55 (1): 54–58.
9. Shivdasani, R.A. 2006. MicroRNAs: Regulators of gene expression and cell differentiation. *Blood* 108 (12): 3646–3653.
10. Meister, G. 2013. Argonaute proteins: Functional insights and emerging roles. *Nature Reviews Genetics* 14 (7): 447–459.
11. Bartel, D.P. 2009. MicroRNAs: Target recognition and regulatory functions. *Cell* 136 (2): 215–233.
12. Sun, L., M. Sun, K. Ma, and J. Liu. 2020. Let-7d-5p suppresses inflammatory response in neonatal rats with necrotizing enterocolitis via LGALS3-mediated TLR4/NF-kappaB signaling pathway. *American Journal of Physiology. Cell Physiology* 319 (6): C967–C979.
13. Zhang, K., X. Zhang, A. Lv, S. Fan, and J. Zhang. 2020. Saccharomyces boulardii modulates necrotizing enterocolitis in neonatal mice by regulating the sirtuin 1/NFkappaB pathway and the intestinal microbiota. *Molecular Medicine Reports* 22 (2): 671–680.
14. Kazgan, N., M.R. Metukuri, A. Purushotham, J. Lu, A. Rao, S. Lee, M. Pratt-Hyatt, A. Lickteig, I.L. Csanaky, Y. Zhao, et al. 2014. Intestine-specific deletion of SIRT1 in mice impairs DCoH2-HNF-1alpha-FXR signaling and alters systemic bile acid homeostasis. *Gastroenterology* 146 (4): 1006–1016.
15. Egan, C.E., C.P. Sodhi, M. Good, J. Lin, H. Jia, Y. Yamaguchi, P. Lu, C. Ma, M.F. Branca, S. Weyandt, et al. 2016. Toll-like receptor 4-mediated lymphocyte influx induces neonatal necrotizing enterocolitis. *The Journal of Clinical Investigation* 126 (2): 495–508.
16. Sodhi, C.P., W.B. Fulton, M. Good, M. Vurma, T. Das, C.S. Lai, H. Jia, Y. Yamaguchi, P. Lu, T. Prindle, et al. 2018. Fat composition in infant formula contributes to the severity of necrotising enterocolitis. *British Journal of Nutrition* 120 (6): 665–680.
17. Good, M., C.P. Sodhi, C.E. Egan, A. Afrazi, H. Jia, Y. Yamaguchi, P. Lu, M.F. Branca, C. Ma, T. Prindle Jr., et al. 2015. Breast milk protects against the development of necrotizing enterocolitis through inhibition of Toll-like receptor 4 in the intestinal epithelium via activation of the epidermal growth factor receptor. *Mucosal Immunology* 8 (5): 1166–1179.
18. Griffiths-Jones, S., Grocock, R.J., van Dongen, S., Bateman, A., Enright, A.J. 2006. miRBase: microRNA sequences, targets and gene nomenclature. *Nucleic Acids Research* 34 (Database issue): D140–144.
19. Griffiths-Jones, S., A. Bateman, M. Marshall, A. Khanna, and S.R. Eddy. 2003. Rfam: An RNA family database. *Nucleic Acids Research* 31 (1): 439–441.
20. Pruesse, E., C. Quast, K. Knittel, B.M. Fuchs, W. Ludwig, J. Peplies, and F.O. Glockner. 2007. SILVA: A comprehensive online resource for quality checked and aligned ribosomal RNA sequence data compatible with ARB. *Nucleic Acids Research* 35 (21): 7188–7196.
21. Bao, W., K.K. Kojima, and O. Kohany. 2015. Repbase Update, a database of repetitive elements in eukaryotic genomes. *Mobile DNA* 6: 11.
22. Robinson, M.D., D.J. McCarthy, and G.K. Smyth. 2010. edgeR: A bioconductor package for differential expression analysis of digital gene expression data. *Bioinformatics* 26 (1): 139–140.
23. Clark, J.A., S.M. Doelle, M.D. Halpern, T.A. Saunders, H. Holubec, K. Dvorak, S.A. Boitano, and B. Dvorak. 2006. Intestinal barrier failure during experimental necrotizing enterocolitis: Protective effect of EGF treatment. *American Journal of Physiology. Gastrointestinal and Liver Physiology* 291 (5): G938-949.
24. Cohran, V., E. Managlia, E.M. Bradford, T. Goretsky, T. Li, R.B. Katzman, P. Cheresh, J.B. Brown, J. Hawkins, S.X.L. Liu, et al. 2016. Epithelial PIK3R1 (p85) and TP53 regulate survivin expression during adaptation to ileocecal resection. *American Journal of Pathology* 186 (7): 1837–1846.
25. Deng, Z., J. Jin, Z. Wang, Y. Wang, Q. Gao, and J. Zhao. 2017. The metal nanoparticle-induced inflammatory response is regulated by SIRT1 through NF-kappaB deacetylation in aseptic loosening. *International Journal of Nanomedicine* 12: 3617–3636.
26. Ong, A.L.C., and T.S. Ramasamy. 2018. Role of Sirtuin1-p53 regulatory axis in aging, cancer and cellular reprogramming. *Ageing Research Reviews* 43: 64–80.
27. de la Torre, Gomez C., R.V. Goreham, J.J. Bech Serra, T. Nann, and M. Kussmann. 2018. "Exosomics"-a review of biophysics,

biology and biochemistry of exosomes with a focus on human breast milk. *Frontiers in Genetics* 9: 92.
28. Patel, A.L., and J.H. Kim. 2018. Human milk and necrotizing enterocolitis. *Seminars in Pediatric Surgery* 27 (1): 34–38.
29. Yu, S., Z. Zhao, L. Sun, and P. Li. 2017. Fermentation results in quantitative changes in milk-derived exosomes and different effects on cell growth and survival. *Journal of Agriculture and Food Chemistry* 65 (6): 1220–1228.
30. Gribar, S.C., C.P. Sodhi, W.M. Richardson, R.J. Anand, G.K. Gittes, M.F. Branca, A. Jakub, X.H. Shi, S. Shah, J.A. Ozolek, et al. 2009. Reciprocal expression and signaling of TLR4 and TLR9 in the pathogenesis and treatment of necrotizing enterocolitis. *The Journal of Immunology* 182 (1): 636–646.
31. Hackam, D.J., M. Good, and C.P. Sodhi. 2013. Mechanisms of gut barrier failure in the pathogenesis of necrotizing enterocolitis: Toll-like receptors throw the switch. *Seminars in Pediatric Surgery* 22 (2): 76–82.
32. Dheer, R., R. Santaolalla, J.M. Davies, J.K. Lang, M.C. Phillips, C. Pastorini, M.T. Vazquez-Pertejo, and M.T. Abreu. 2016. Intestinal epithelial toll-like receptor 4 signaling affects epithelial function and colonic microbiota and promotes a risk for transmissible colitis. *Infection and Immunity* 84 (3): 798–810.
33. Yazji, I., C.P. Sodhi, E.K. Lee, M. Good, C.E. Egan, A. Afrazi, M.D. Neal, H. Jia, J. Lin, C. Ma, et al. 2013. Endothelial TLR4 activation impairs intestinal microcirculatory perfusion in necrotizing enterocolitis via eNOS-NO-nitrite signaling. *Proceedings of the National Academy of Sciences of the United States of America* 110 (23): 9451–9456.
34. Jantscher-Krenn, E., M. Zherebtsov, C. Nissan, K. Goth, Y.S. Guner, N. Naidu, B. Choudhury, A.V. Grishin, H.R. Ford, and L. Bode. 2012. The human milk oligosaccharide disialyllacto-N-tetraose prevents necrotising enterocolitis in neonatal rats. *Gut* 61 (10): 1417–1425.
35. Good, M., C.P. Sodhi, Y. Yamaguchi, H. Jia, P. Lu, W.B. Fulton, L.Y. Martin, T. Prindle, D.F. Nino, Q. Zhou, et al. 2016. The human milk oligosaccharide 2'-fucosyllactose attenuates the severity of experimental necrotising enterocolitis by enhancing mesenteric perfusion in the neonatal intestine. *British Journal of Nutrition* 116 (7): 1175–1187.
36. van Herwijnen, M.J.C., T.A.P. Driedonks, B.L. Snoek, A.M.T. Kroon, M. Kleinjan, R. Jorritsma, C.M.J. Pieterse, E. Hoen, and M.H.M. Wauben. 2018. Abundantly present miRNAs in milk-derived extracellular vesicles are conserved between mammals. *Frontiers in Nutrition* 5: 81.
37. Simpson, M.R., G. Brede, J. Johansen, R. Johnsen, O. Storro, P. Saetrom, and T. Oien. 2015. Human breast milk miRNA, maternal probiotic supplementation and atopic dermatitis in offspring. *PLoS One* 10 (12): e0143496.
38. Izumi, H., M. Tsuda, Y. Sato, N. Kosaka, T. Ochiya, H. Iwamoto, K. Namba, and Y. Takeda. 2015. Bovine milk exosomes contain microRNA and mRNA and are taken up by human macrophages. *Journal of Dairy Science* 98 (5): 2920–2933.
39. Gu, Y., M. Li, T. Wang, Y. Liang, Z. Zhong, X. Wang, Q. Zhou, L. Chen, Q. Lang, Z. He, et al. 2012. Lactation-related microRNA expression profiles of porcine breast milk exosomes. *PLoS One* 7 (8): e43691.
40. Chen, T., Q.Y. Xi, R.S. Ye, X. Cheng, Q.E. Qi, S.B. Wang, G. Shu, L.N. Wang, X.T. Zhu, Q.Y. Jiang, et al. 2014. Exploration of microRNAs in porcine milk exosomes. *BMC Genomics* 15: 100.
41. Ma, J., C. Wang, K. Long, H. Zhang, J. Zhang, L. Jin, Q. Tang, A. Jiang, X. Wang, S. Tian, et al. 2017. Exosomal microRNAs in giant panda (Ailuropoda melanoleuca) breast milk: Potential maternal regulators for the development of newborn cubs. *Science and Reports* 7 (1): 3507.
42. Valadi, H., K. Ekstrom, A. Bossios, M. Sjostrand, J.J. Lee, and J.O. Lotvall. 2007. Exosome-mediated transfer of mRNAs and microRNAs is a novel mechanism of genetic exchange between cells. *Nature Cell Biology* 9 (6): 654–659.
43. Xie, M.Y., L.J. Hou, J.J. Sun, B. Zeng, Q.Y. Xi, J.Y. Luo, T. Chen, and Y.L. Zhang. 2019. Porcine milk exosome MiRNAs attenuate LPS-induced apoptosis through inhibiting TLR4/NF-kappaB and p53 pathways in intestinal epithelial cells. *Journal of Agriculture and Food Chemistry* 67 (34): 9477–9491.